

REPRINTED FROM:

The Mechanics and Biophysics of Hearing (Lecture Notes in Biomathematics Vol. 87)

Edited by P. Dallos, C. D. Geisler, J. W. Matthews, M. A. Ruggero, and C. R. Steele
(Springer-Verlag, 1990).

THE FRACTAL DOUBLY STOCHASTIC POISSON POINT PROCESS AS A MODEL FOR THE COCHLEAR NEURAL SPIKE TRAIN

Malvin C. Teich, Robert G. Turcott, and Steven B. Lowen

*Department of Electrical Engineering, Columbia University, and
Fowler Memorial Laboratory, Columbia College of Physicians & Surgeons,
New York, NY 10027, USA*

Introduction

It has been shown that the neural spike trains transmitted along primary fibers in the cochlear nerve can be described by a dead-time-modified fractal point process (Teich, 1989). These spike trains manifest highly irregular firing rates, irregularly shaped pulse-number distributions (even when the number of samples is large), and fractional power-law behavior in the Fano-factor time curve with a fractional power-law exponent that appears to depend on the level of stimulation (Teich and Khanna, 1985; Teich and Turcott, 1988; Teich, Johnson, Kumar and Turcott, 1990).

This fractal behavior is not manifested over short time scales (< 100 msec), so it will not be revealed by certain types of measurements, such as pulse-interval distributions and post-stimulus time histograms. Point-process models based on such measures may therefore be used with confidence only for modeling short-term effects. Indeed, the dead-time-modified Poisson point process model (Cox, 1962) has achieved its success in this domain.

In this paper we show that a particular type of fractal point process that we have developed, the dead-time-modified fractal doubly stochastic Poisson point process (FDSPP), exhibits behavior that is consistent with all of the experimental statistics of spontaneous and pure-tone driven VIIIth-nerve action potentials examined to date. FDSPPs are generally not members of the renewal family of processes; rather, they are generated as a result of long-term fractal correlations. Particular attention is devoted to two specific examples of this process: the fractal-shot-noise-driven (FSND) DSPP and one of its special cases, the fractal-Gaussian-noise-driven (FGND) DSPP (Lowen and Teich, 1989, 1990). This particular process can arise from physiologically plausible nerve-spike generation models, as indicated briefly at the end of this paper.

Because refractoriness in the auditory nerve, as elsewhere in the nervous system, has both absolute and relative components (Teich and Diament, 1980; Teich, 1985), it is appropriate to modify the FDSPP by "sick time" rather than dead time. Nevertheless, a suitable approximation is provided by dead time

(Prucnal and Teich, 1983), particularly since our principal interest lies in phenomena with time scales > 100 msec. All of the processes described in this paper are therefore modified by dead time, although for simplicity this will not be explicitly stated.

Identification of the Neural Point Process

The sequence of action potentials recorded from spontaneously firing and driven adult-cat high-frequency auditory nerve fibers has been used to construct a number of experimental measures, including the pulse-interval distribution (PID), pulse-number distribution (PND), Fano-factor time curve (FFC), serial count correlation coefficient (SCC), and normalized range (R/S). The collection of these statistics provides a rather comprehensive picture of the underlying neural spike train and enables us to make reasonable conjectures about the point process that describes these events (Teich, Turcott and Lowen, 1990).

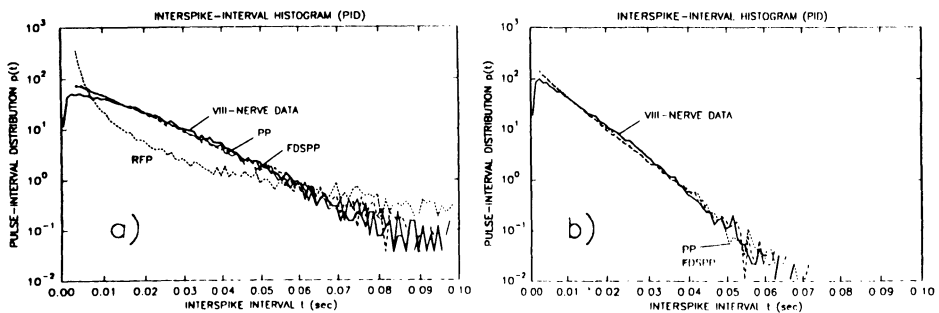


FIGURE 1 a) Pulse-interval distribution (PID) for 405 sec of data from a spontaneously firing high-frequency auditory nerve fiber (Unit A) with mean interspike interval $\langle t \rangle = 15.3$ msec and dead time $\tau_d \approx 3$ msec (solid curve). Also shown are the results of simulations for three theoretical models, all of which incorporate a fixed dead time: the Poisson point process (PP), the renewal fractal point process (RFP), and the fractal doubly stochastic Poisson point process (FDSPP). The model parameters are chosen to give approximately the same mean interspike interval and refractoriness as the data. Additional parameters used in the RFP simulation are $\alpha = 0.7$ and $t_c = 100$ sec. These values were selected so that the point process would exhibit fractal behavior over the time scales of interest, and yet avoid excessively large intervals which leads to computational difficulty in estimating the various statistical measures. Additional parameters used in the FDSPP simulation are $\alpha = 0.65$ and $t_f = 400$ msec. The PP and the FDSPP fit the data, but the RFP does not. b) PID for 800 sec of data for this same fiber, but now in response to a pure-tone stimulus applied at the characteristic frequency (CF) of the unit. The mean interspike interval $\langle t \rangle = 8.9$ msec and the dead time $\tau_d \approx 2$ msec (solid curve). The reduced mean interevent time is reflected in the greater negative slope on this semi-logarithmic plot. The PID for the RFP closely resembles that shown in a) and is therefore not illustrated. Again the simulated FDSPP (modified by fixed dead time), with model parameters chosen to give approximately the same mean interspike interval, refractoriness, fractal dimension ($\alpha = 0.86$), and fractal onset time ($t_f = 40$ msec) as the data, provides a good fit.

The PID, PND, and FFC are, by now, well-known statistics that have been described in detail elsewhere (Teich and Khanna, 1985; Teich and Turcott, 1988; Teich, 1989). The SCC and R/S provide estimates of the degree of serial correlation in the data set. The SCC gives the correlation between the numbers of neural spikes in adjacent counting periods, and is generally a function of the counting time T . The R/S measure reflects correlations among collections of large numbers of interspike intervals. It has the advantage of being a valid measure even when the data exhibit extremely long-term correlations, as well as large (or infinite) variance; these are characteristics that can cause a process to appear nonstationary and are consequently deleterious to standard measures (Mandelbrot, 1983).

We have compared these experimental statistics with those predicted by several theoretical models, including a dead-time-modified Poisson point process (PP), a dead-time-modified renewal fractal point process (RFP), and a dead-time-modified fractal doubly stochastic Poisson point process (FDSPP). We have performed simulations using various forms of this latter process, and found that both the FSND-DSPP and the FGND-DSPP exhibit behavior that accords with all of these statistics. The PP and RFP, in contrast, do not.

The PP is well-known. As shown in Fig. 1, it gives rise to PIDs that agree well with both spontaneous and driven data. However, as illustrated for spontaneous firings in Fig. 2, its PND ($T=1$ sec) is narrower than that of the data, while its FFC and SCC remain flat for large times rather than increasing with T , and rescaled range analysis leads to the $k^{1/2}$ law rather than the steeper curve that describes the data. The PP fails to describe the driven data in the same way.

Because the RFP is less well-known, we provide a brief discussion of its behavior. A renewal point process with interevent times governed by the hyperbolic distribution is invariant to certain scaling transformations (Mandelbrot, 1965), and therefore exhibits fractal characteristics. Its pulse-interval distribution $p(t)$ is

$$p(t) = \begin{cases} A t^{-u}, & \tau_d \leq t \leq \tau_c \\ 0, & \text{otherwise} \end{cases} \quad (1)$$

The quantity A normalizes the distribution, and is a function of the other parameters. As shown in Fig. 1, its PID exhibits a reduction of interspike intervals with values near the mean and a concurrent enhancement of long and short intervals, relative to that of the Poisson. Because of its renewal and fractal nature, we refer to this process as the renewal fractal point process (RFP).

Such large-variance interspike intervals can lead to long-term spike correlations. Even though the interspike intervals of the RFP are independent, the numbers of spikes occurring in successive counting periods of fixed time T are not. For example, with the decreased proportion of intermediate interspike intervals, given a low number of spikes in a particular counting period we know with high probability that this period fell within a long interspike interval. Because of this the following counting period is also likely to fall within the same interspike interval, and is therefore also likely to register a low number of

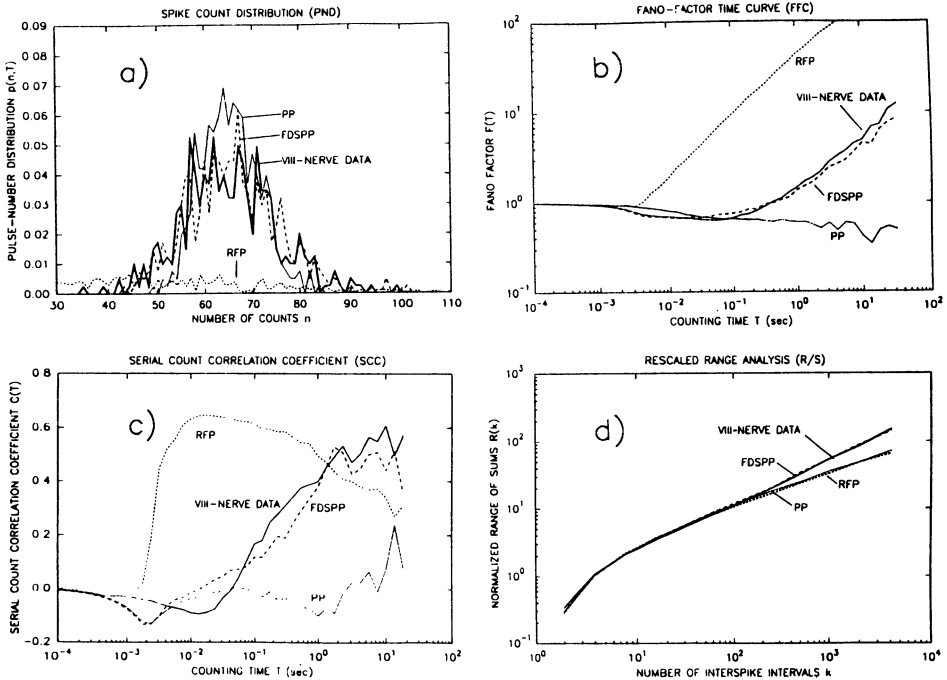


FIGURE 2 a) Pulse-number distribution (PND) constructed from the same spontaneous spike train as the PID shown in Fig. 1a, using a counting time $T = 1$ sec (solid curve). The PND is the probability $p(n, T)$ of observing n spikes in the observation time T , versus the number of spikes n . PNDs from simulations of the three theoretical models are also shown. The model parameters are chosen to give the same mean count as the data. The PND obtained from the FDSPP resembles the data. On the other hand, the PND obtained from the PP is narrower than the data while that obtained from the RFP is far broader than the data. b) The Fano-factor time curve (FFC) is constructed from the PND; it is the ratio of the count variance to the count mean for different counting times T . For VIII-nerve data, $F(T)$ typically grows in power-law fashion as T^a ($0 < a < 1$) for sufficiently large counting times, implying a power-law normalized coincidence rate and a power-law form for the power spectral density at low frequencies (Teich, 1989). Again the FFC obtained from the FDSPP resembles the data quite closely whereas the FFCs of the PP and the RFP deviate substantially from it, even though the latter does exhibit power-law behavior. c) The serial count correlation coefficient (SCC) gives the correlation between the numbers of neural spikes in adjacent counting periods, and is in general a function of T . For the PP, $a = 0$ so that $C(T) = 0$ as is evident in the figure for sufficiently large counting times (the dip in the curve in the vicinity of 2 msec, which arises from dead time, would be moderated were sick time used instead). Once again the SSC obtained from the FDSPP closely resembles the data while the SSCs associated with the PP and the RFP deviate substantially from it. In the domain of counting times where the Fano-factor time curve behaves as T^a , $C(T)$ plateaus at the value $2^a - 1$ as required by the relation between these parameters. d) Whereas the SCC reflects correlations between successive counts, the RS parameter reflects correlations among interspike intervals. This measure is obtained by first estimating the interval mean and standard deviation in a block of interspike intervals of size k . For each of the k intervals, the difference between the value of the interval and the mean value is obtained and the result is successively added to a cumulative sum. The range is defined as the difference between the maximum and minimum values achieved within the cumulative sum, and this is normalized by the sample standard deviation to give $R(k)$. The normalized range of sums $R(k)$ is estimated for increasing values of k and plotted against k . With $R(k)$ proportional to k^h , $h > 0.5$ indicates positive correlation, $h < 0.5$ indicates negative correlation, and $h = 0.5$ indicates uncorrelated intervals (Hurst, 1951; Feller, 1951). The renewal nature of the PP and RFP cause $R(k)$ to behave as $k^{1/2}$; the data and the results from the FDSPP rise more steeply, indicating positive correlation for collections of large numbers of interspike intervals.

spikes. On the other hand, if a large number of spikes is registered in a particular counting period, it is unlikely that this counting period contains a long interspike interval and, since short interspike intervals are far more likely, it is highly probable that the following spike number will also be large. Indeed, sample functions of this point process have a strongly clustered appearance. Expanding the time scale surrounding a cluster of spikes generally reveals subclusters. For the Poisson process, on the other hand, the exponential nature of the interevent-time distribution, along with the independence of successive intervals, guarantees that the spike counts are independent.

The independence of the interspike intervals of the RFP leads to the same R/S behavior as the Poisson, as is evident in Fig. 2d. At the same time, the correlation among successive counts is apparent in the serial count correlation coefficient shown in Fig. 2c. It is this correlation that gives rise to the very broad pulse-number distribution shown in Fig. 2a and a Fano-factor time curve that increases with T in power-law fashion, as illustrated in Fig. 2b. As is evident from Figs. 1 and 2, the RFP does not model the data well.

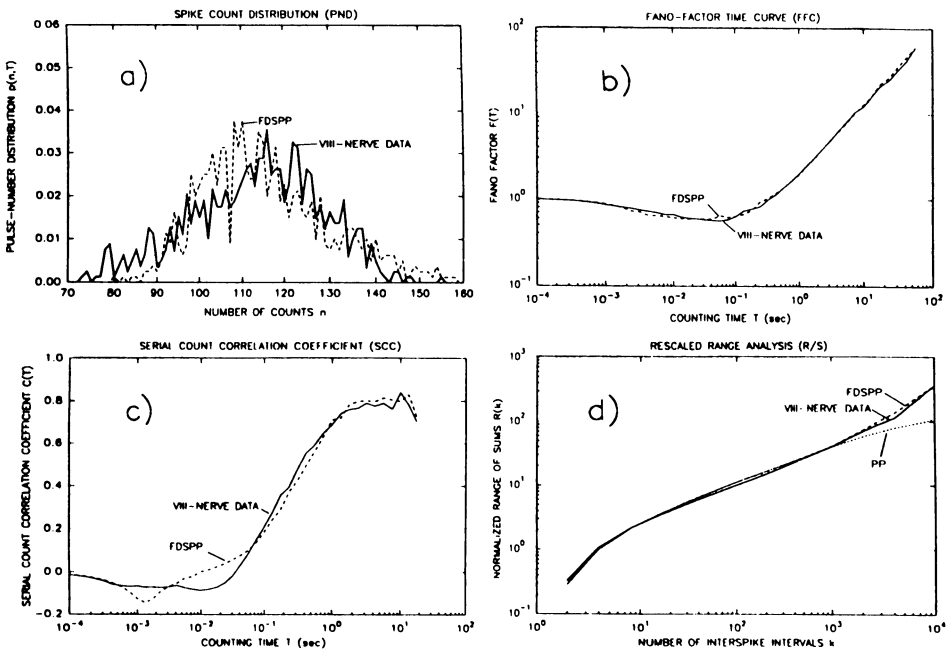


FIGURE 3 a) PND ($T = 1$ sec), b) FFC, c) SCC, and d) R/S constructed from the same 800-sec driven spike train as that used in Fig. 1b for the PID. The renewal processes are not represented since their behavior is similar to that presented in Fig. 2. The fractal dimension revealed by the slope of the FFC curve is approximately $\alpha = 0.86$, which is greater than the value observed in Fig. 2b for spontaneous firing ($\alpha = 0.65$). The increased FFC exponent is reflected in a larger count-correlation estimate, as is evident in the SCC curve (compare with Fig. 2c). The increase in α and $C(T)$ under stimulation has been observed in all VIII-nerve fibers examined to date. All of the measures constructed from a simulated FDSPP, with the same parameters as reported in Fig. 1b, resemble the neural-spike data quite closely.

In contrast, the FDSPP, and in particular the FSND-DSPP and the FGND-DSPP, give results that are largely indistinguishable from the experimental statistics that we have examined both for spontaneous firings (Fig. 2) and for driven firings (Fig. 3), and we identify it as the point process that characterizes the auditory neural spike train (Teich, Turcott and Lowen, 1990). Its behavior arises from long-term fractal rate correlations which can be removed by randomly shuffling the interspike intervals, as shown in Figs. 4 and 5 for spontaneous and driven data respectively.

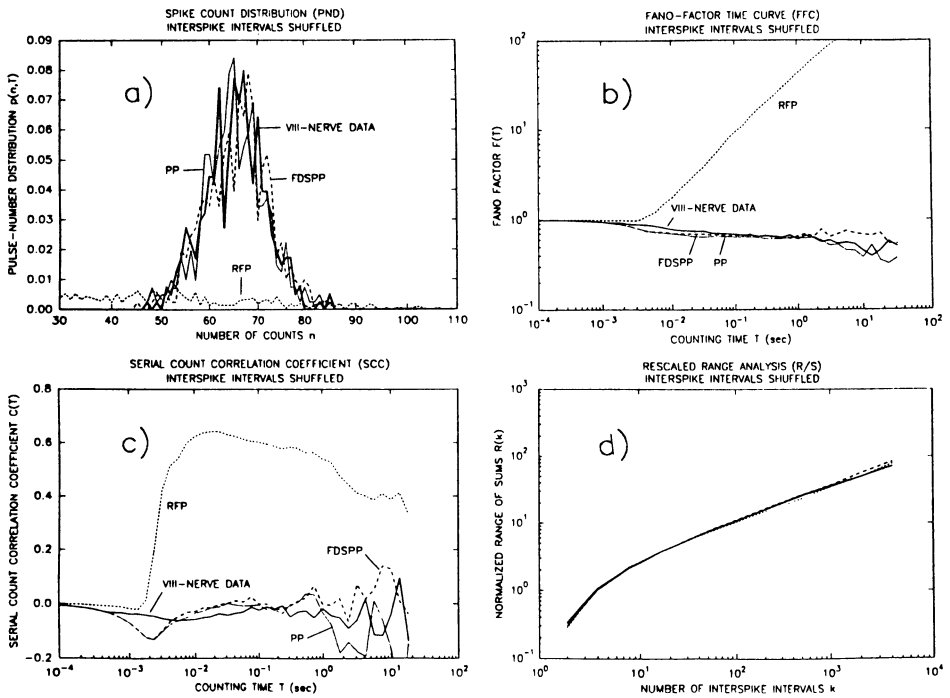


FIGURE 4 Same as Fig. 2 (spontaneous firings) except that the interspike intervals were randomly shuffled for both the experimental and simulated spike trains before constructing these measures. Several observations merit mention. First, measures constructed from the PP and RFP are not altered by shuffling. This is as expected since both are renewal processes which, by definition, have independent and identically distributed interspike intervals. Second, measures constructed from the VIII-nerve data are altered substantially by shuffling, which provides unequivocal evidence that the auditory neural events are not describable by a renewal process. Third, measures constructed from the FDSPP behave in the same way as measures constructed from the data, providing additional evidence that it is a good model for the neural point process. Finally, the results for the data and the FDSPP are indistinguishable from those of the PP after random shuffling. The shuffling removes the long-term fractal rate correlations, leaving a residue of intrinsically irreducible fluctuations, which is simply the dead-time-modified homogeneous Poisson point process. This result is consistent with the data provided in Fig. 1a where it was demonstrated that the PID for the VIII-nerve data, the FDSPP, and the PP are essentially the same.

It is of interest to note that the FFC exponent α (i.e., the fractal dimension) increases when the unit is driven, as does the serial count correlation coefficient for long counting times as reflected in the SCC curve. All of the VIII-nerve fibers we have examined to date, when presented with pure-tone stimuli, reveal an increase in the value of the fractal dimension, correlation coefficient, and firing rate (Teich, Johnson, Kumar and Turcott, 1990).

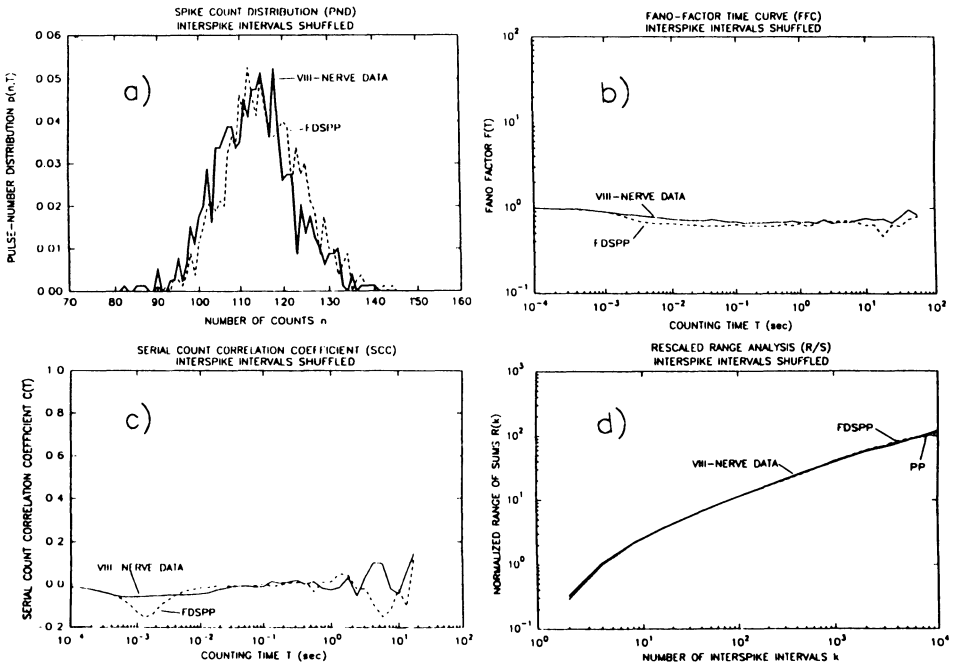


FIGURE 5 Same as Fig. 3 (driven firings) except that the interspike intervals were randomly shuffled for both the experimental and simulated spike trains before constructing these measures. As with the spontaneous data, measures constructed from the VIII-nerve data are altered substantially by shuffling, which provides confirming evidence that the auditory neural events are not describable by a renewal process. Measures constructed from the FDSPP behave in the same way as those constructed from the data, so that this model appears to be suitable for describing the neural point process in the presence of a pure-tone stimulus as well as in its absence. The shuffled results for both the data and the simulation are indistinguishable from those of a Poisson point process since shuffling the intervals is similar to generating a renewal point process using the PID, and the PID of both the data and the FDSPP are approximately exponential.

On Possible Origins of the Fractal Behavior

The underlying fractal behavior of the VIII-nerve spike train could originate at any of a number of peripheral loci (Teich, 1989) including nonlinear cellular vibrations in the Organ of Corti (Teich, Khanna and Keilson, 1989), chaotic oscillations of the membrane potential, neurotransmitter diffusion, and fractal ionic channel openings and closings. The FDSPP turns out to be useful for modeling several of these possibilities.

Acknowledgment

This work was supported by the National Science Foundation.

References

- Cox, D.R. (1962) *Renewal Theory*. Methuen, London.
- Feller, W. (1951) The asymptotic distribution of the range of sums of independent random variables. *Ann. Math. Stat.* 22, 427-432.
- Hurst, H.E. (1951) Long-term storage capacity of reservoirs. *Trans. Amer. Soc. Civil Eng.* 116, 770-808.
- Lowen, S.B. and Teich, M.C. (1989) Generalised $1/f$ shot noise. *Electron. Lett.* 25, 1072-1074.
- Lowen, S.B. and Teich, M.C. (1991) Fractal shot-noise-driven doubly stochastic Poisson point process. Submitted for publication.
- Mandelbrot, B.B. (1965) Self-similar error clusters in communication systems and the concept of conditional stationarity. *IEEE Trans. Commun. Tech.* 13, 71-90.
- Mandelbrot, B.B. (1983) *The Fractal Geometry of Nature*. Freeman, New York.
- Prucnal, P.R. and Teich, M.C. (1983) Refractory effects in neural counting processes with exponentially decaying rates. *IEEE Trans. Syst. Man Cybern.* SMC-13, 1028-1033.
- Teich, M.C. (1985) Normalizing transformations for dead-time-modified Poisson counting distributions. *Biol. Cybern.* 53, 121-124.
- Teich, M.C. (1989) Fractal character of the auditory neural spike train. *IEEE Trans. Biomed. Eng.* 36, 150-160.
- Teich, M.C. and Diamant, P. (1980) Relative refractoriness in visual information processing. *Biol. Cybern.* 38, 187-191.
- Teich, M.C. and Khanna, S.M. (1985) Pulse-number distribution for the neural spike train in the cat's auditory nerve. *J. Acoust. Soc. Am.* 77, 1110-1128.
- Teich, M.C. and Turcott, R.G. (1988) Multinomial pulse-number distributions for neural spikes in primary auditory fibers: Theory. *Biol. Cybern.* 59, 91-102.
- Teich M.C., Khanna, S.M., and Keilson, S.E. (1989) Nonlinear dynamics of cellular vibrations in the organ of Corti. *Acta Otolaryngologica Suppl.* 467, 265-279.
- Teich, M.C., Johnson, D.H., Kumar, A.R., and Turcott, R.G. (1990) Rate fluctuations and fractional power-law noise recorded from cells in the lower auditory pathway of the cat. *Hear. Res.* 46, 41-52.
- Teich, M.C., Turcott, R.G., and Lowen, S.B. (1990) Identification of the point process characterizing the auditory neural spike train. *Assoc. Res. Otolaryngol. Abst.* 155, 141.